纳 米 光 子 学 丛 书

Nanoscale Photonics and Spectroscopy

纳米光子学与光谱

（第2版）

孙萌涛　程宇清　崔　琳　著
Sun Mengtao　Cheng Yuqing　Cui Lin

清華大學出版社
北 京

内 容 简 介

本书系统介绍了纳米尺度下光子学和光谱学的基本物理原理，以及它们的相互作用机制。还介绍了金属表面等离激元的激发、探测和对分子光谱的增强机制，其中包括表面等离基元增强的吸收、荧光、拉曼、光学成像等。此外，还揭示了表面等离基元和激子耦合相互作用的物理机制，进一步阐释了这种相互作用在表面催化反应中的应用。

本书结构完整，物理原理阐述清晰，列举的应用例子是最新的科学前沿研究。本书适合作为研究生和高年级本科生的光学教材，也可作为相关领域科研工作者的基础参考书。

图书在版编目(CIP)数据

纳米光子学与光谱＝Nanoscale Photonics and Spectroscopy. Ⅱ：英文/孙萌涛，程宇清，崔琳著. —2版. —北京：清华大学出版社，2023.11

（纳米光子学丛书）

ISBN 978-7-302-64762-1

Ⅰ. ①纳… Ⅱ. ①孙… ②程… ③崔… Ⅲ. ①纳米技术—光子—英文 Ⅳ. ①TB383 ②O572.31

中国国家版本馆 CIP 数据核字(2023)第 193945 号

责任编辑：鲁永芳
封面设计：常雪影
责任校对：王淑云
责任印制：刘海龙

出版发行：清华大学出版社
网　　址：http://www.tup.com.cn，http://www.wqbook.com
地　　址：北京清华大学学研大厦 A 座　　邮　　编：100084
社 总 机：010-83470000　　邮　　购：010-62786544
投稿与读者服务：010-62776969，c-service@tup.tsinghua.edu.cn
质量反馈：010-62772015，zhiliang@tup.tsinghua.edu.cn
印 装 者：涿州汇美亿浓印刷有限公司
经　　销：全国新华书店
开　　本：170mm×240mm　　**印　　张**：29.25　　**字　　数**：489 千字
版　　次：2019 年 10 月第 1 版　2023 年 11 月第 2 版　　**印　　次**：2023 年 11 月第1 次印刷
定　　价：129.00 元

产品编号：103032-01

《纳米光子学丛书》
编　委　会

CONTENTS

CHAPTER 1

Introduction

All the color figures please scan the QR code.

1.1 Concept of Spectroscopy

Spectroscopy is the study of the interaction between matter and electromagnetic radiation(Spectrum + copy). In 1672, Isaac Newton described an experiment in which he permitted sunlight to pass through a small hole and then through a prism(Fig. 1-1). Newton found that sunlight, which looks white to us, is actually made up of a mixture of all the colors of the rainbow.

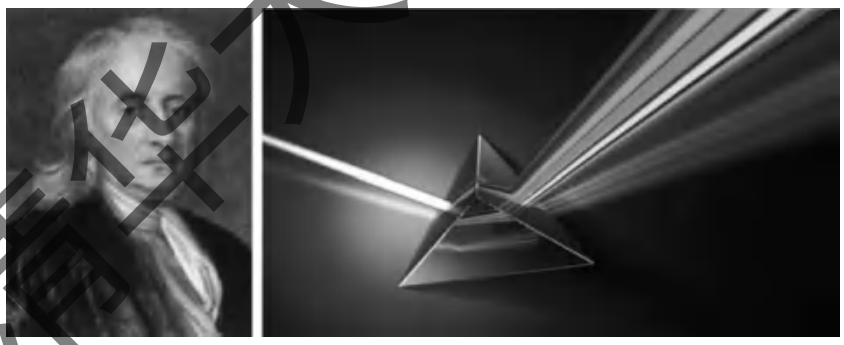

Fig. 1-1 Isaac Newton and his experiment
(For colored figure please scan the QR code on page 1)

In 1802, William Hyde Wollaston built an improved spectrometer that included a lens to focus the sun's spectrum on a screen(Fig. 1-2). Upon use, Wollaston realized that the colors were not spread uniformly, but instead had

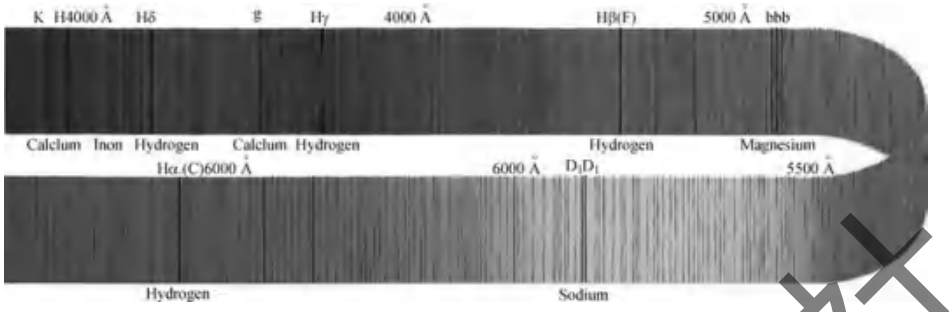

Fig. 1-2 Lines in the solar spectrum. The range illustrated is from 3900 Å to 6900 Å
(For colored figure please scan the QR code on page 1)

missing patches of colors, which appeared as dark bands in the spectrum. In 1815, Joseph Fraunhofer also examined the solar spectrum, and found about 600 such dark lines (missing colors), which are now known as Fraunhofer lines, or absorption lines.

Spectroscopy is the study of the interaction between matter and electromagnetic radiation. The entire electromagnetic spectrum is shown in Fig. 1-3.

In molecular spectroscopy, a Jablonski diagram (Fig. 1-4) is used to illustrate the electronic states of a molecule and the transitions between them. The states are arranged vertically by energy and grouped horizontally by spin multiplicity. Nonradiative transitions are indicated by squiggly arrows and radiative transitions by straight arrows. The vibrational ground states of each electronic state are indicated with thick lines, the higher vibrational states with thinner lines[1]. The diagram is named after Aleksander Jabłoński[2].

Radiative transitions involve the absorption, if the transition occurs to a higher energy level, or the emission, in the reverse case, of a photon. Nonradiative transitions arise through several different mechanisms, all differently labeled in the diagram. Relaxation of the excited state to its lowest vibrational level is called vibrational relaxation. This process involves the dissipation of energy from the molecule to its surroundings, and thus it cannot occur for isolated molecules. A second type of nonradiative transition is internal conversion (IC), which occurs when a vibrational state of an electronically

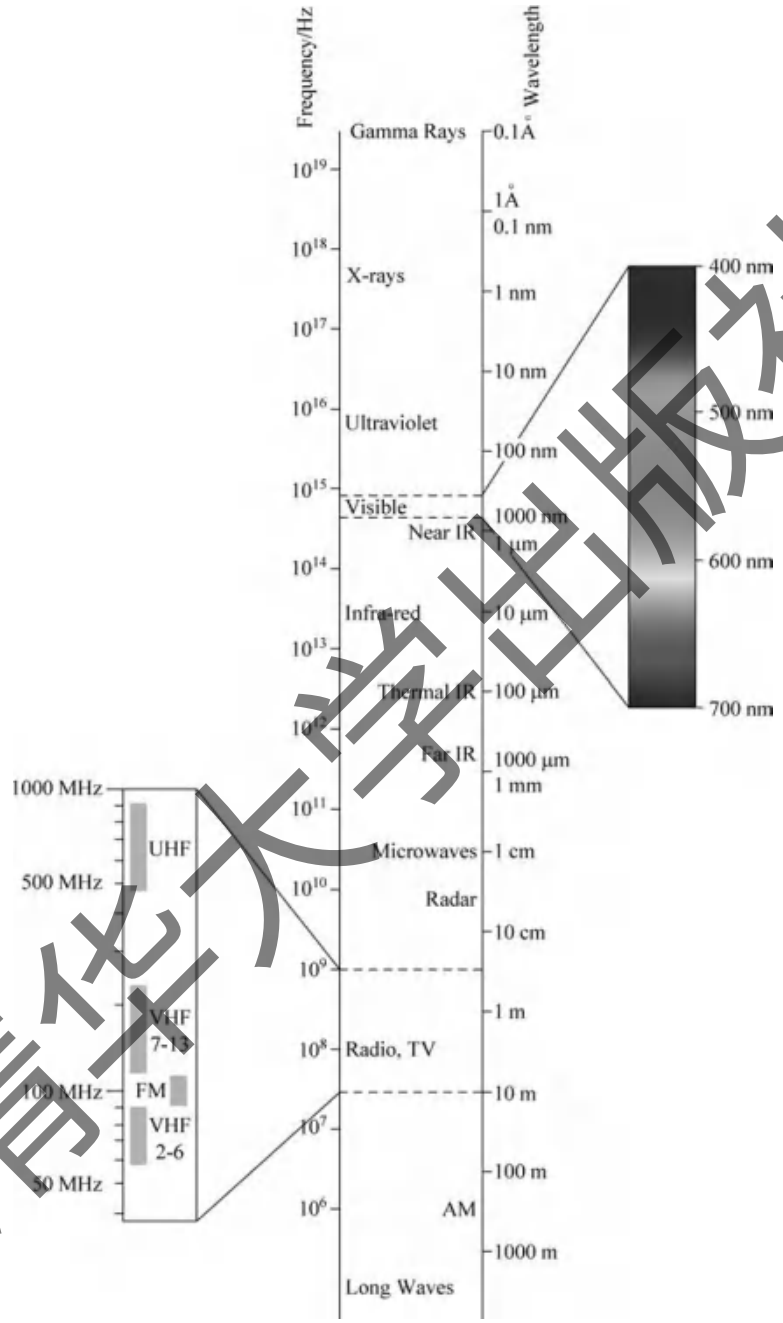

Fig. 1-3 The entire electromagnetic spectrum

(For colored figure please scan the QR code on page 1)

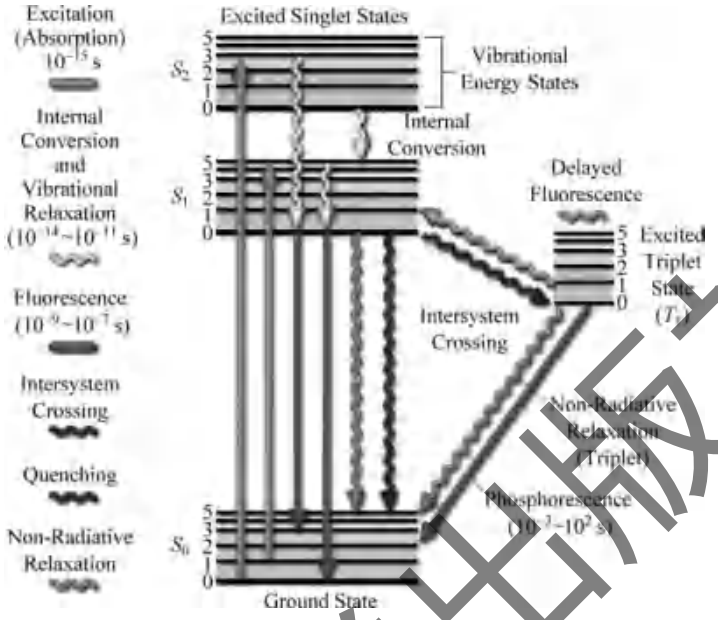

Fig. 1-4 Jablonski(energy)diagram

(For colored figure please scan the QR code on page 1)

excited state can couple to a vibrational state of a lower electronic state. A third type is intersystem crossing(ISC); this is a transition to a state with a different spin multiplicity. In molecules with large spin-orbit coupling, ISC is much more important than in molecules that exhibit only small spin-orbit coupling. ISC can be followed by phosphorescence.

1.2 Concept of Photonics and Plasmonics

The word "photonics" is derived from the Greek word "phos" meaning light (which has genitive case "photos" and in compound words the root "photo-" is used). Photonics is the physical science of light(photon)generation, detection, and manipulation through emission, transmission, modulation, signal processing, switching, amplification, and detection/sensing. Photonics is closely related to optics. Classical optics long preceded the discovery that light is

quantized, when Albert Einstein famously explained the photoelectric effect in 1905. Optics tools include the refracting lens, the reflecting mirror, and various optical components and instruments developed throughout the 15th to 19th centuries. Key tenets of classical optics, such as Huygens principle, developed in the 17th century, Maxwell's equations and the wave equations, developed in the 19th century, do not depend on quantum properties of light. Photonics is related to quantum optics, optomechanics, electro-optics, optoelectronics, and quantum electronics. However, each area has slightly different connotations by scientific and government communities and in the marketplace. Quantum optics often connotes fundamental research, whereas photonics is used to connote applied research and development. Photonics also relates to the emerging science of quantum information and quantum optics. The science of photonics includes investigation of the emission, transmission, amplification, detection, and modulation of light.

In photonics, metals are not usually thought of being very useful, perhaps except mirrors. In most cases, metals are strong absorbers of light, a consequence of their large free-electron density. However, in the miniaturization of photonic circuits, it is now being realized that metallic structures can provide unique ways of manipulating light at length scales smaller than the wavelength. Maxwell's equations tell us that an interface between a dielectric (e. g. silica glass) and a metal (e. g. Ag or Au) can support an surface plasmon (SP). An SP is a coherent electron oscillation that propagates along the interface together with an electromagnetic wave. These unique interface waves result from the special dispersion characteristics (dependence of dielectric constant on frequency) of metals. Similar to photonics, by means of SPs, suchresearch is referred to as plasmonics, which can be considered as optics at the nanoscale[3].

What distinguishes SPs from "regular" photons is that they have a much smaller wavelength at the same frequency. For example, a HeNe laser, whose free-space emission wavelength is 633 nm, can excite an SP at a Si/Ag interface with a wavelength of only 70 nm. When the laser frequency is tuned very close

to the SP resonance, SP wavelengths in the nanometer range can be achieved. The short-wavelength SPs enable the fabrication of nanoscale optical integrated circuits, in which light can be guided, split, filtered, and even amplified using plasmonic integrated circuits that are smaller than the optical wavelength.

SPs are easily accessible excitations in metals and semiconductors and involve a collective motion of the conduction electrons. These excitations can be exploited to manipulate electromagnetic waves at optical frequencies("light") in new ways that are unthinkable in conventional dielectric structures. The field of surface plasmon nanophotonics is rapidly developing and impacting a wide range of areas including: electronics, photonics, chemistry, biology, and medicine. SPs are coherent delocalized electron oscillations that exist at the interface between any two materials where the real part of the dielectric function changes sign across the interface(e.g. a metal-dielectric interface, such as a metal sheet in air). The existence of surface plasmons was first predicted in 1957 by Rufus Ritchie[4]. Schematic representation of an electron density wave propagating along a metal-dielectric interface can be seen from Fig. 1-5. The charge motion in a surface plasmon always creates electromagnetic fields outside(as well as inside)the metal. The charge density oscillations and associated electromagnetic fields are called SPP waves. The exponential dependence of the electromagnetic field intensity on the distance away from the interface is shown on the right in Fig. 1-5[5]. These waves can be excited very efficiently with light in the visible range of the electromagnetic spectrum.

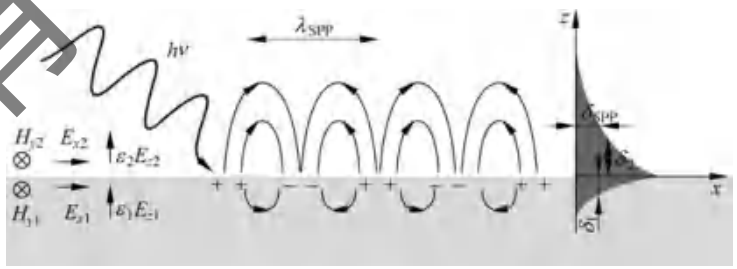

Fig. 1-5 Schematic representation of an electron density wave propagating along a metal-dielectric interface

(For colored figure please scan the QR code on page 1)

Surface plasmon polaritons (SPPs) are infrared (IR) or visible-frequency electromagnetic waves that travel along a metal-dielectric or metal-air interface. The term "SPP" explains that the wave involves both charge motion in the metal ("surface plasmon") and electromagnetic waves in the air or dielectric ("polariton")[6]. SPPs can be excited by electrons or photons. Excitation by electrons is created by firing electrons into the bulk of a metal. As the electrons scatter, energy is transferred into the bulk plasma. The component of the scattering vector parallel to the surface results in the formation of a SPP[7]. For a photon to excite an SPP, both must have the same frequency and momentum. However, for a given frequency, a free-space photon has less momentum than an SPP because the two have different dispersion relations. This momentum mismatch is the reason that a free-space photon from air cannot couple directly to an SPP. For the same reason, an SPP on a smooth metal surface cannot emit energy as a free-space photon into the dielectric(if the dielectric is unfform). The coupling of photons into SPPs can be achieved using a coupling medium such as a prism or grating or a defect on the metal surface to match the photon and SPP wave vectors(and thus match their momenta). The SPP is a non-radiative electromagnetic surface wave that propagates in a direction parallel to the negative permittivity/dielectric material interface.

Dispersion curve for SPPs can be seen from Fig. 1-6. At low frequency, an SPP approaches a Sommerfeld-Zenneck wave, where the dispersion relation (between frequency and wavevector)is the same as in free space. At a higher frequency, the dispersion relation bends over and reaches an asymptotic limit called the "surface plasma frequency"[8-9]. SPPs are usually shorter in wavelength than the incident light(photons). Hence, SPPs can have tighter spatial confinement and higher local field intensity. Perpendicular to the interface, they have subwavelength-scale confinement. An SPP will propagate along the interface until its energy is lost either to absorption in the metal or

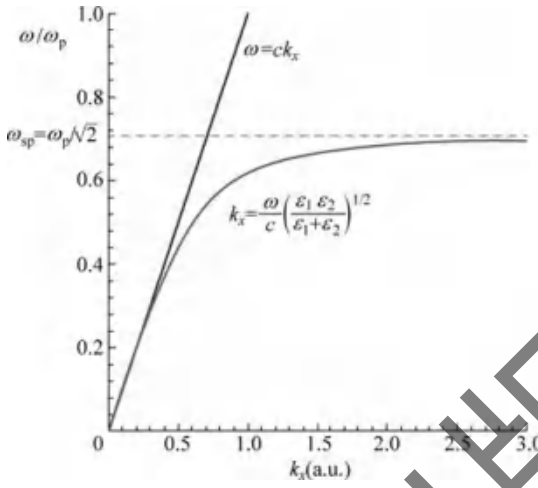

Fig. 1-6 Dispersion curve for SPPs. At low k, the surface plasmon curve (red) approaches the photon curve (blue)
(For colored figure please scan the QR code on page 1)

scattering into other directions (such as into free space). The k is a complex wave vector, $k_x = k'_x + ik''_x$, and in the case of a lossless SPP, it turns out that the x components are real and the z components are imaginary—the wave oscillates along the x direction and exponentially decays along the z direction.

As an SPP propagates along the surface (Fig. 1-5), it loses energy to the metal due to absorption. It can also lose energy due to scattering into free space or into other directions. The intensity of the surface plasmon decays with the square of the electric field, so at a distance x, the intensity has decreased by a factor of $\exp(2k''_x x)$. The propagation length is defined as the distance for the SPP intensity to decay by a factor of 1/e. This condition is satisfied at a length, $L = \frac{1}{2k''_x}$ [10]. The electric field falls off evanescently perpendicular to the metal surface. At low frequencies, the SPP penetration depth into the metal is commonly approximated using the skin depth formula. In the dielectric, the field will fall off far more slowly. The decay lengths in the

metal and dielectric medium can be expressed as, $Z_i = \frac{\lambda}{2\pi}\left(\frac{|\varepsilon_1'| + \varepsilon_2}{\varepsilon_i^2}\right)^{1/2}$, where λ is the wavelength, ε_1' is the real part of the dielectric function of a metal, ε_2 is the permittivity of the dielectric, and i indicates the medium of propagation[10]. SPPs are very sensitive to slight perturbations within the skin depth and, therefore, are often used to probe inhomogeneities of a surface.

The charge motion in a surface plasmon always creates electromagnetic fields outside(as well as inside)the metal. The total excitation, including both the charge motion and associated electromagnetic field, is called as either a SPP at a planar interface, or a localized surface plasmon(LSP)for the closed surface of a small particle. A LSP is the result of the confinement of a surface plasmon in a nanoparticle of size comparable to or smaller than the wavelength of light used to excite the plasmon, see Fig. 1-7(a). The LSP has two important effects: electric fields near the particle's surface are greatly enhanced and the particle's optical absorption has a maximum at the plasmon resonant frequency. The enhancement falls off quickly with distance from the surface and, for noble metal nanoparticles, the resonance occurs at visible wavelengths[10]. Surface plasmon resonance(SPR)is the resonant oscillation of conduction electrons at the interface between the negative and the positive permittivity material stimulated by incident light. LSPRs(localized SPRs)are collective electron charge oscillations in metallic nanoparticles that are excited by light. They exhibit enhanced near-field amplitude at the resonance wavelength. This field is highly localized at the nanoparticle and decays rapidly away from the nanoparticle/dielectric interface into the dielectric background, though the far-field scattering by the particle is also enhanced by the resonance. Light intensity enhancement is a very important aspect of LSPRs and localization means the LSPR has very high spatial resolution (subwavelength), limited only by the size of nanoparticles. Peaks of LSPRs can be well manipulated by the nanostructures, see Fig. 1-7(b)[11].

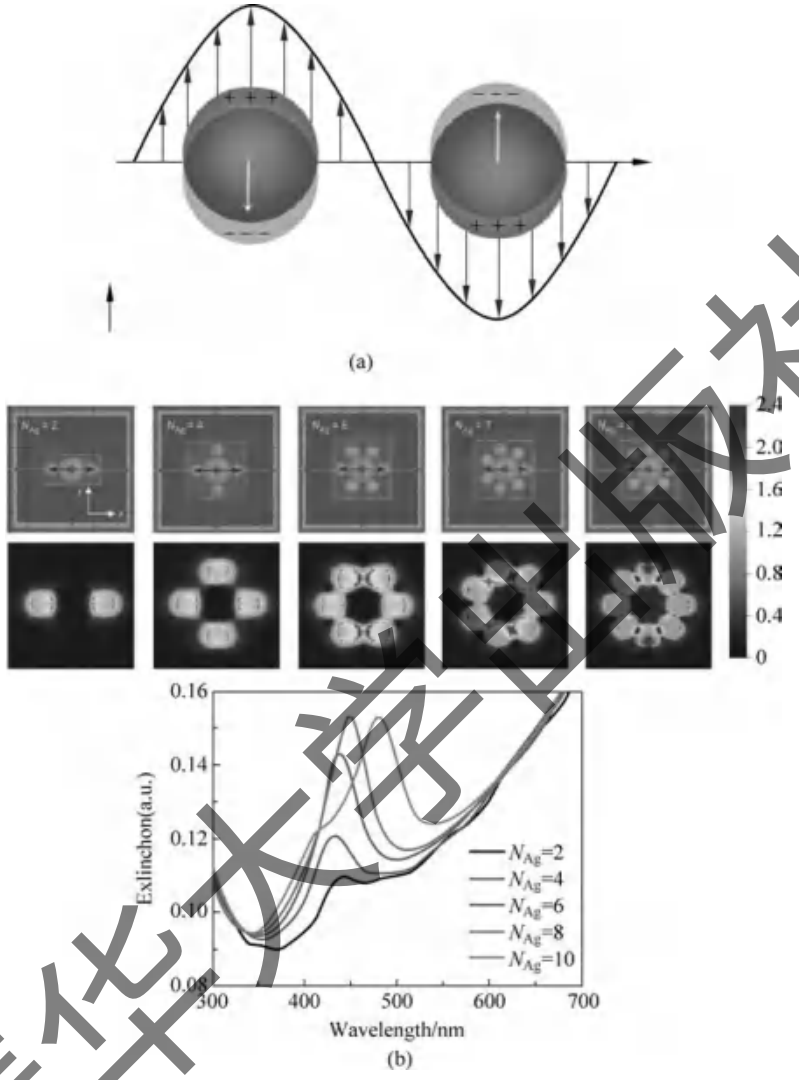

Fig. 1-7 (a) Local surface plasmon, and (b) local surface plasmon resonance by nanoparticles (For colored figure please scan the QR code on page 1)

1.3 Concept of Plasmon-Enhanced Spectroscopy

1.3.1 Plasmon-enhanced fluorescence

The plasmon-enhanced nonlinear optical microscopy of g-C_3N_4 was studied by using the multiple surface plasmon resonances (MSPRs) of the Au @ Ag

nanorods, see Fig. 1-8 in subfigure (a)[12]. The scanning election microscapy (SEM) images of the plasmonic Au@Ag nanorods; and (b)～(d) demonstrate that the Au@Ag nanorods are successfully synthesized, and a silver shell is coated onto each Au nanorod with a thickness of around 10 nm. Compared with the Au nanorods, the resonance peaks at 910 nm and 520 nm indicate a blue shift to 800 nm and 500 nm for the Au@Ag nanorods, and a new resonance peak at 400 nm can be obtained. The plasmon-enhanced two-photon-excited fluorescence (TPEF) of g-C_3N_4 covered with the Au@Ag nanorods was first studied (Fig. 1-9)[12]. According to the absorption and

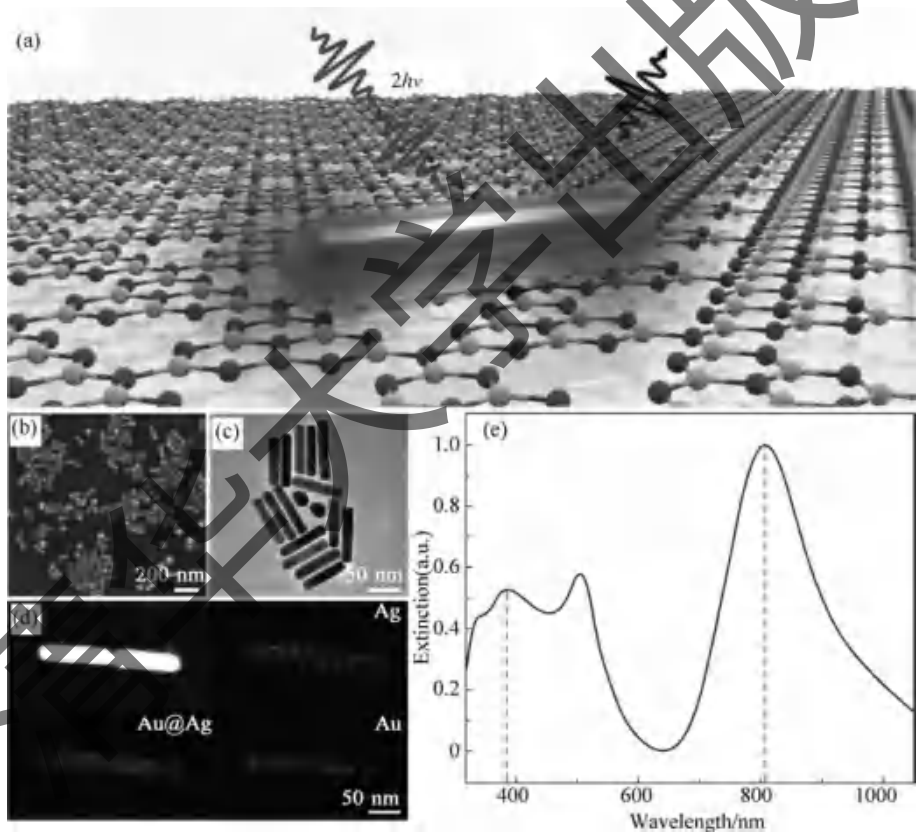

Fig. 1-8 Characterization and optical properties of Au@Ag nanorods

(a) Plasmon-enhanced nonlinear optical microscopy of g-C_3N_4 by the Au@Ag nanorods; (b) and (c) The SEM and TEM images of the Au@Ag nanorods, and (d) The elemental mapping images of the two Au@Ag nanorods; (e) UV-visible spectra of the chemically synthesized Au@Ag nanorods

(For colored figure please scan the QR code on page 1)

photoluminescence (PL) spectra of g-C_3N_4 shown in Fig. 1-9 (b), a strong extinction peak can be observed around 400 nm, which matches the fundamental frequency at 800 nm of the incident light. The TPEF images of g-C_3N_4 without (Fig. 1-9(c)) and with (Fig. 1-9(d)) the Au@Ag nanorods were obtained by 800 nm excitation. By using strong MSPRs at 800 nm and 400 nm, the TPEF can be strongly enhanced via the Au@Ag nanorods covering on the g-C_3N_4 surface.

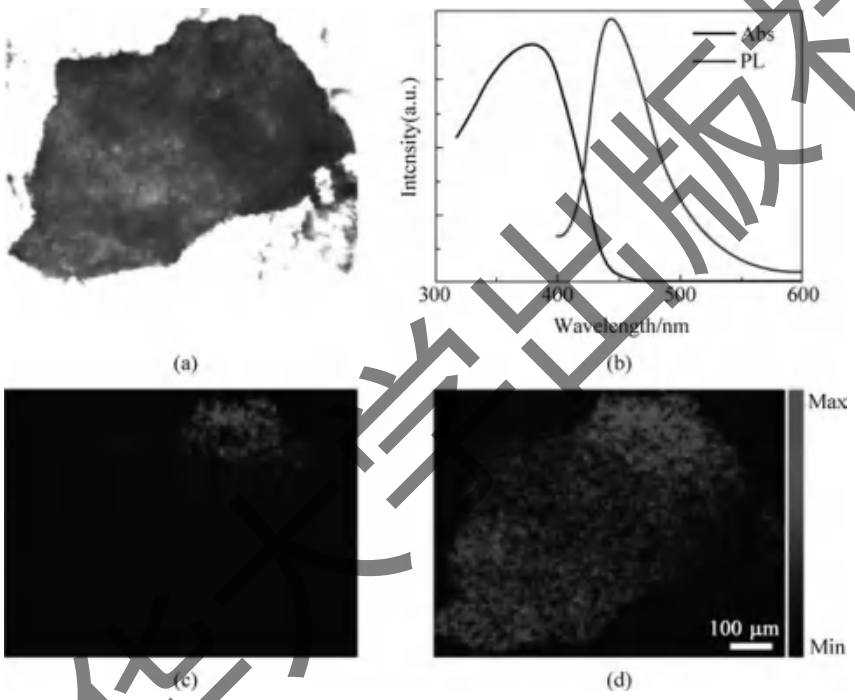

Fig. 1-9 Optical characterization of g-C_3N_4

(a) The bright field optical image of g-C_3N_4; (b) The absorption and PL spectra of g-C_3N_4; (c) The TPEF and (d) Plasmon-enhanced TPEF of g-C_3N_4 without and with the Au@Ag nanorods, respectively

(For colored figure please scan the QR code on page 1)

1.3.2 Plasmon-enhanced Resonance fluorescence energy transfer

Ozel firstly reports the mechanism of the independent control about plasmon coupling to donor or acceptor. They select Au MNPs and CdTe QDs which were assembled by layer-by-layer assembly technique[13]. They made experiments about

the plasmon only coupling with donor or acceptor QDs(Fig. 1-10(a)～(c)). Note that there is a strong spectral overlap(Fig. 1-10(d)) when the FRET condition is satisfied[14].

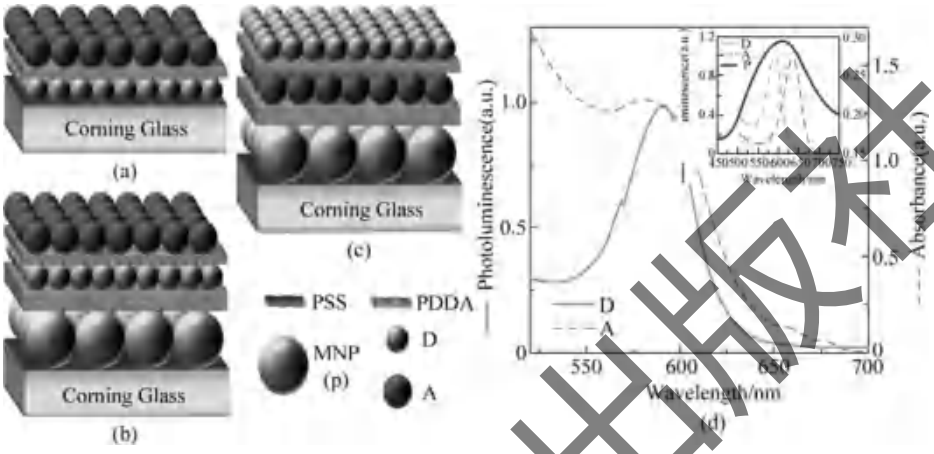

Fig. 1-10 (a)～(c) The conventional FRET, the plasmon-mediated FRET with plasmon coupling only to the donor QDs, and the plasmon-mediated FRET with plasmon coupling only to the acceptor QDs, respectively; (d) The PL spectrum
(For colored figure please scan the QR code on page 1)

In a concerned donor-acceptor system, a comparison was made between the PL spectra of steady states about the plasmon-enhanced donor(pD-A)(see Fig. 1-11(a) and (b)) and the plasmon-enhanced acceptor (D-pA)(see Fig. 1-11(c) and (d)). It is concluded that FRET is occurred during D-A in two cases. For the D-pA, there is not FRET, but an fluorescence enhancement for A, as well as pA; for the pD-A, it has FRET and enhanced fluorescence of D almost all transfer to A[13].

1.3.3 Surface-enhanced Raman scattering

Since the discovery of SERS[15], it has been extensively studied experimentally and theoretically because of its extremely high surface sensitivity and powerful application on fingerprint vibrational spectroscopy in qualitative and quantitative analysis. The pyridine molecule is an important probe molecule in

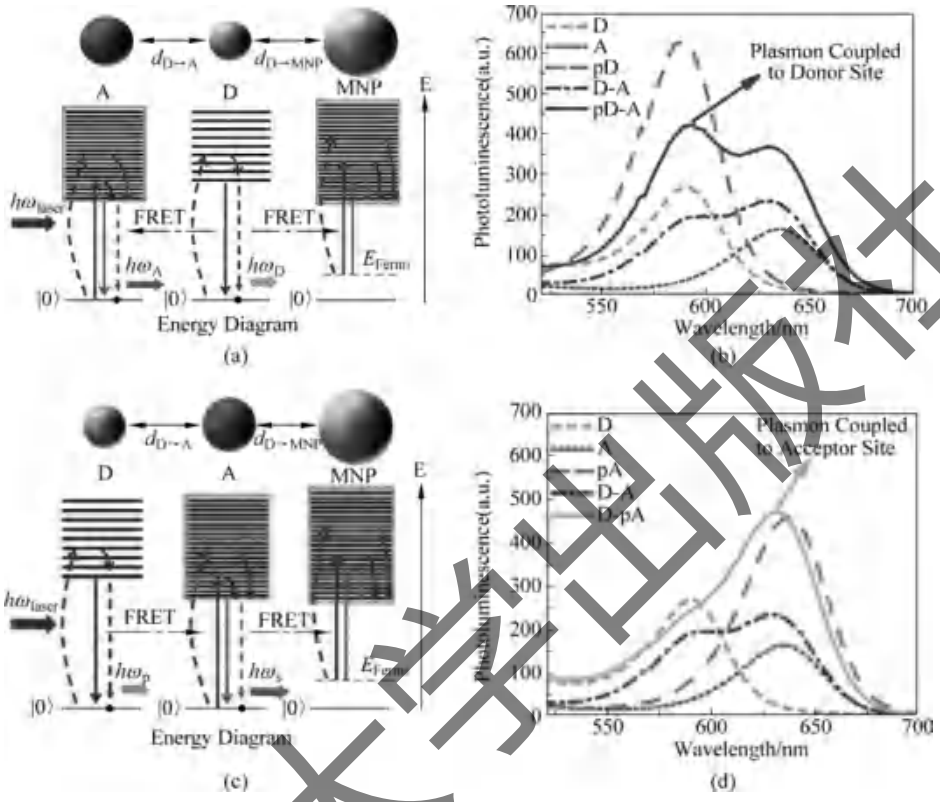

Fig. 1-11 Plasmon-Acceptor'Exciton coupling[13]

(For colored figure please scan the QR code on page 1)

SERS field, and the enhancement effect is strongly dependent on the SERS substrates[16]. In Fig. 1-12, (a) is the absorption spectroscopy of pyridine adsorbed on Au @ Pd substrate, it can be found that most of electrons and holes are distributed on the first layer of the substrate. (b) demonstrate that chemical enhancement can enhance Raman spectra of pyridine about 10 times. (c) reveals that electromagnetic enhancement can reach up to 10^3, where the distance of two nanoparticles is 2 nm; and the (d) reveals that electromagnetic enhancement is strongly dependent on the distance of nanoparticles. The total enhancements, including chemical and electromagnetic enhancements, are up to 10^4, which is consistent with the experimental reports[17].

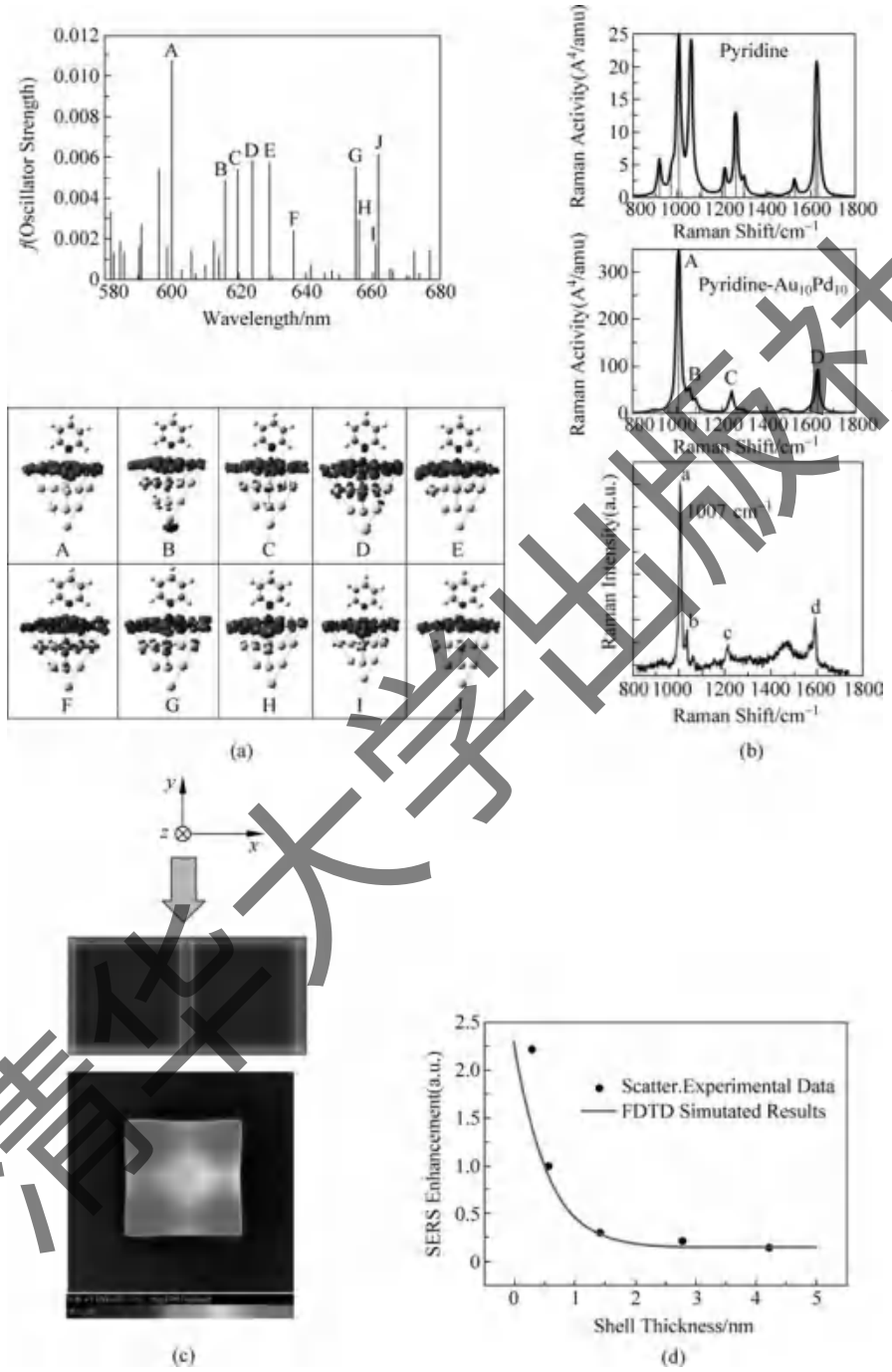

Fig. 1-12 The chemical and electromagnetic enhancements on pyridine adsorbed on the Au@Pd substrate

(For colored figure please scan the QR code on page 1)

1.3.4 The remote-excitation of SERS

Currently, the plasmonic waveguide has been successfully applied in the field of remote-excitation surface-enhanced Raman spectroscopy[18-21]. Compared with traditional SERS, remote excitation SERS has many advantages. In normal SERS, the excited light is focused on the detected spot, which is called local SERS. In contrast, in the "remote SERS", the excited spot is far away from the detected target, which is excited by the SPPs with a "remote mode". Ag or Au waveguides offer a way to go below the size limit because they transfer optical signals via SPPs. The SPPs can propagate along the metal waveguide and emit free photons at imperfections or at the end of waveguide, while some of them are lost due to the ohmic damping. The energy transfer from the spot of illumination and the hot-spot can be supported mainly by the remote systems based on plasmonic waveguide, as illustrated in Fig. 1-13(A)[19]. The SPPs could of course excite the nanoscale hot-spot remotely, which can avoid the strong background noise because of a large area of the excited spot, and isolate heat effects from the area of excited light to the target excited in the area of sub-diffraction wavelength. Morcover, it can reduce the possibility of the sample damage by high laser excitation.

Based on surface-enhanced spectroscopy, a novel way of sensing measurements can be provided by such a remote SERS system, see Fig. 1-13(A), and it can be used in systems where normal SERS is unsuitable, such as Raman detection of biomolecules in living cells[18-22]. In 2014, Ujii et al. reported the remote excitation SERS by plasmonic waveguide in living cell[22]. As shown in Fig. 1-13(B), the plasmonic hotspot(at the gap of two Ag nanowires(NWs), or of NW and nanoparticles) on the Ag NW probe inserted into the cells was excited by SPPs, and the signals were collected from the other side the Ag NW probe outside the cells. A clear remote SERS spectrum can be observed by using an Ag NW probe hotspot inserted into a living HeLa cell[22].

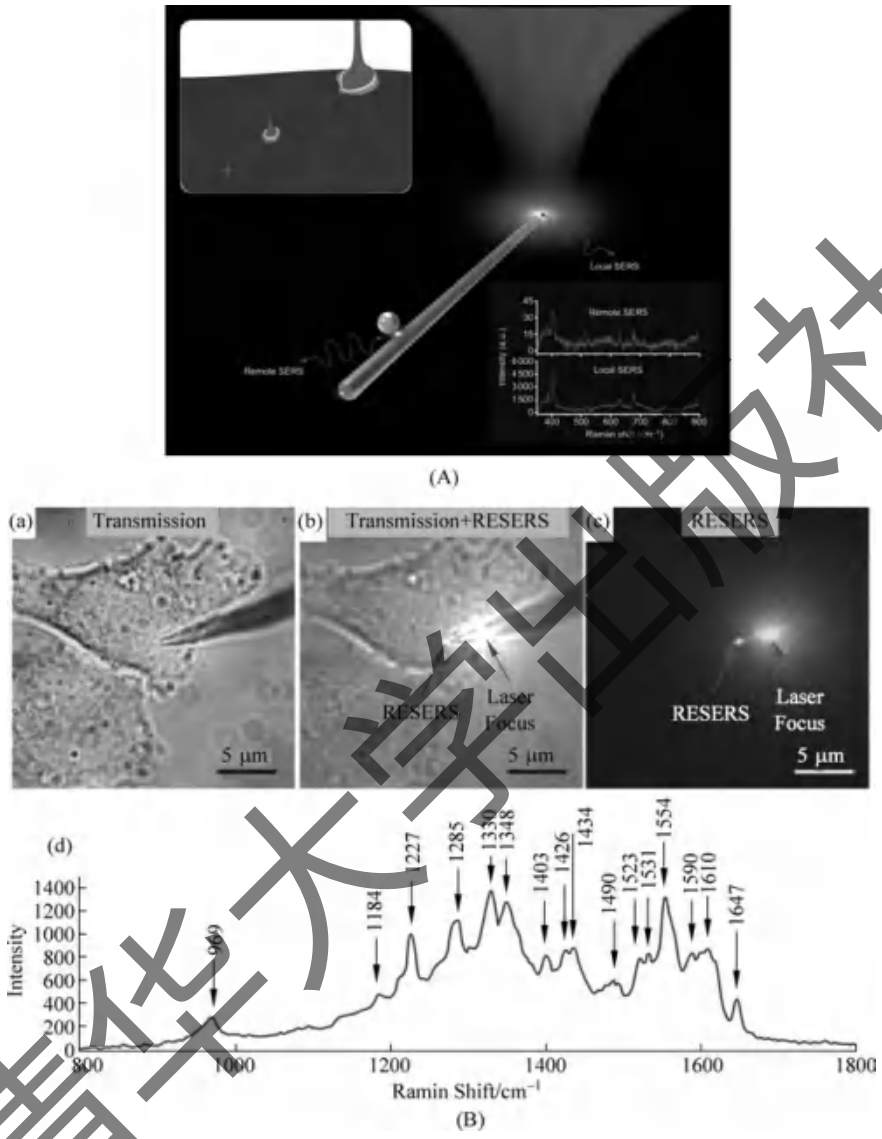

Fig. 1-13 (A) A sketch of the local SERS and the remote SERS in an Ag NP-NW system(Raman molecule adsorbed on the Ag NW). The Raman signals obtained at the illuminating terminal are local SERS, while the signals collected at the junction whose energy come from the propagating SPPs are remote SERS. (B) Scheme of the positions chosen for remote-excitation SERS spectroscopy inside a live HeLa cell during Ag NW probe endoscopy

(a)~(c) Remote excitation SERS endoscopy of a live HeLa cell. (a) Optical transmission; (b) Combination of optical transmission and remote excitation SERS; (c) Remote excitation SERS only images of an Ag NW probe in a live HeLa cell; (d) A remote excitation SERS spectrum from the nucleus of the live HeLa cell

(For colored figure please scan the QR code on page 1)

1.3.5 Tip-enhanced Raman scattering spectroscopy

Tip-enhanced Raman scattering(TERS), the combination of scanning probe microscopy (SPM) with surface-enhanced Raman spectroscopy, was first reported in 2000[23]. This technique has subsequently attracted a great deal of attention. Several groups have built TERS systems based on an atomic force microscope(AFM)or scanning tunneling microscope(STM)[24-26]. The distance between the tip and the film can be precisely controlled in both these SPM techniques, allowing fine adjustment during enhancement studies. Additionally, both techniques can provide resolution at the atomic scale, allowing researchers to "see clearly" target molecules. Figure 1-14 demonstrates the plasmon-driven chemical reaction in high-vacuum tip-enhanced TERS(HV-TERS)[26].

1.3.6 Remote excitation-TERS microscopy

Figure 1-15 demonstrates the Remote excitation-TERS[27]. Subfigures (a) and (b) show TERS spectra observed under direct excitation using *p* and *s* polarization, respectively, with a laser power of 50 kW/cm^2. The Raman peaks at 700 cm^{-1}, 999 cm^{-1}, 1023 cm^{-1}, 1072 cm^{-1}, and 1572 cm^{-1} are resolved in the spectra, which can be assigned to the vibrational modes of C-H out-of-plane deformation, a mixture of S-H bending and in-plain ring deformation, in-plane ring deformation, a mixture of C-S stretching and in-plane ring deformation, and C-C stretching of benzenethiol, respectively. It was found that both the Raman and background intensities were higher with *p*-polarization than with *s*-polarization, resulting from the excitation of gap-mode plasmons between the apex of the Ag NW and the Au(111) substrate. Conversely, with remote excitation this polarization dependence was reversed. (c) and (d) show TERS spectra observed under remote excitation with *p*-and *s*-polarization, respectively, using the same laser power(50 kW/cm^2). The spectra in (c) and

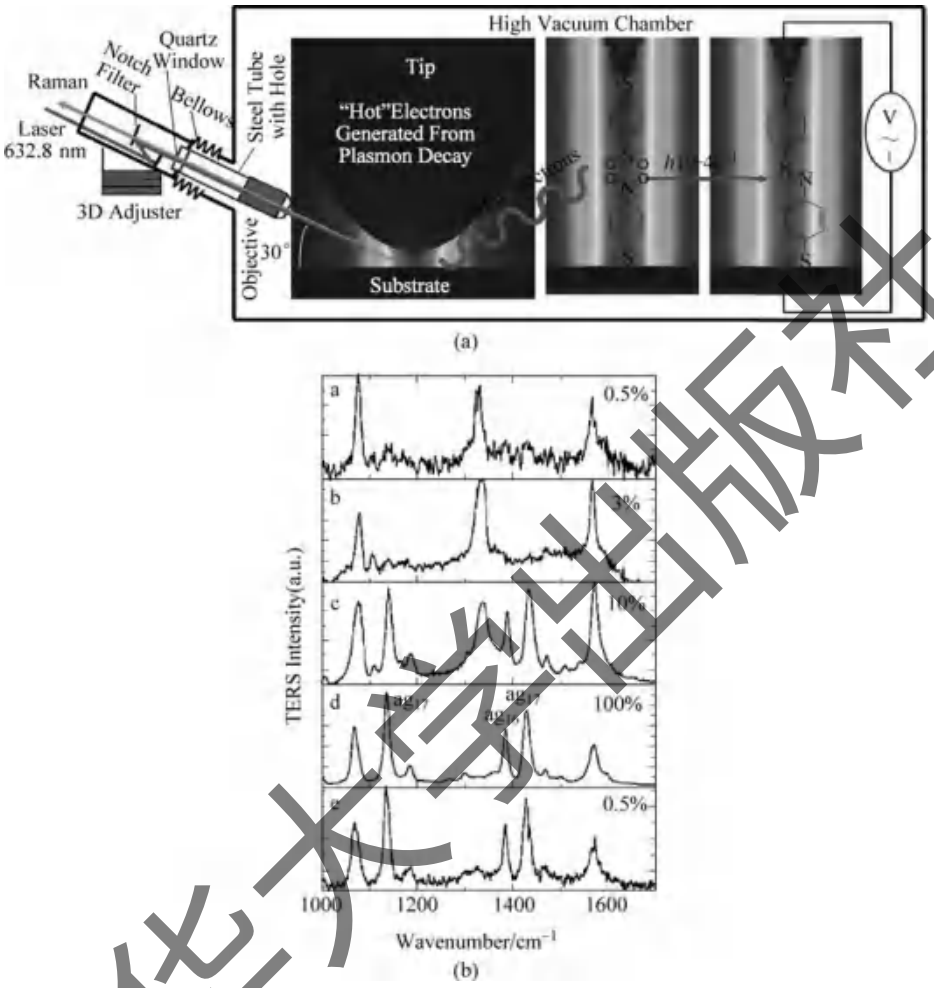

Fig. 1-14 The plasmon-driven chemical reaction in HV-TERS

(a) The scheme of set up and experimental details, and (b) The processes of the plasmon-driven chemical reaction

(For colored figure please scan the QR code on page 1)

(d) are multiplied by 10 times for easier comparison. Note that, with remote excitation, when the laser power is above 100 kW/cm^2, the remote-TERS signal tends to fluctuate and indeed sometimes the NW was cut at the focused spot. This could be due to a temperature rise at the NP/NW junction upon laser irradiation. Here, both the Raman and background intensities were higher with *s*-polarization than with *p*-polarization. This is in line with expectation,

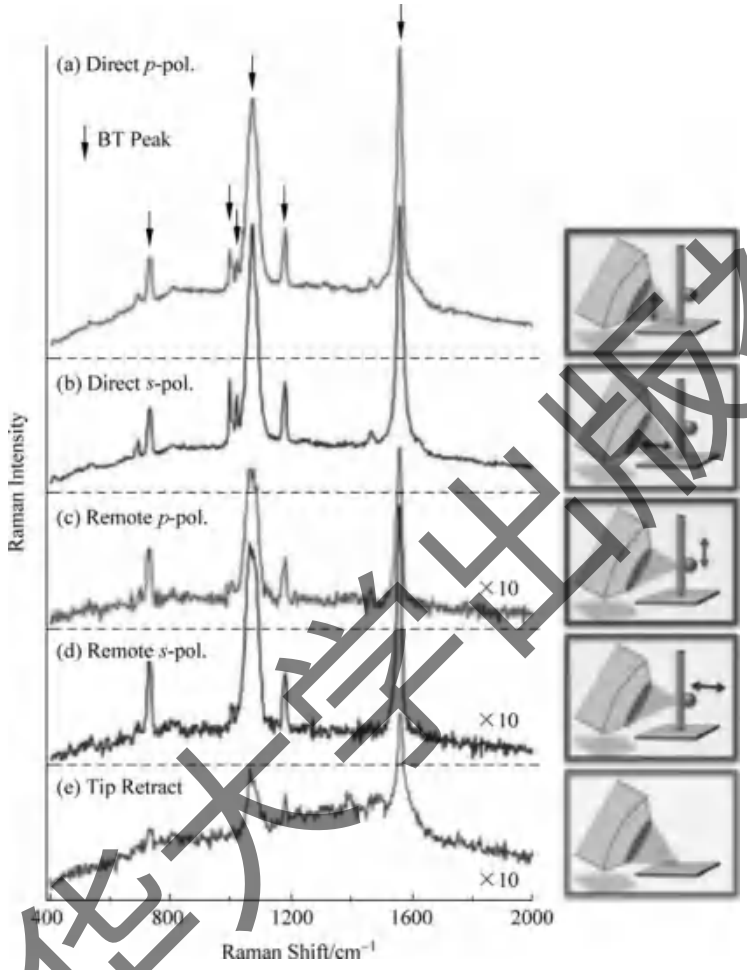

Fig. 1-15 Raman spectrum from benzenethiol-modified Au(111) substrate in the presence(a)～(d), and the absence of the tip(e). (a) and (b) TERS spectra measured when HeNe laser light (632.8 nm, 50 kW/cm^2) is focused at the end of a Ag NW with *p*-and *s*-polarization (direct excitation), respectively. (c) and (d) TERS spectra measured when the laser light is focused at the Au NP with *p*-and *s*-polarization (remote excitation), respectively. The tip is approached to the substrate under shear-force AFM feedback. Spectra shown in(c)～(e) are multiplied 10 times for easier comparison. Raman peaks that are assigned to Raman scattering of benzenethiol are indicated by an arrow in(a)

(For colored figure please scan the QR code on page 1)